ELSEVIER

Experimental Thermal and Fluid Science 24 (2001) 1–9

Experimental Thermal and Fluid Science

www.elsevier.nl/locate/etfs

Measurements of the gas-particle convective heat transfer coefficient in a packed bed for high-temperature energy storage

Emmanuel C. Nsofor [a,*], George A. Adebiyi [b]

[a] *Department of Mechanical Engineering and Energy processes, Southern Illinois University, Carbondale, IL 62901-6603, USA*
[b] *Department of Mechanical Engineering, Mississippi State University, Mississippi State, MS 39762, USA*

Received 6 June 2000; received in revised form 5 September 2000; accepted 5 October 2000

Abstract

Experimental measurements of the forced convection gas-particle heat transfer coefficient in a packed bed, high-temperature, thermal energy storage system were performed using a custom-made experimental facility. Special attention was paid to the application of uncertainty analysis (a very important concept in experimentation). General and detailed uncertainty analyses were carried out, which identified the choices that were made in the experimental planning and procedure to ensure reliable final results. The experimental data reduction program used the governing equations and the results of the uncertainty analysis while making allowance for media property variations with temperature. Results were correlated in terms of Nusselt number, Prandtl number and Reynolds number and comparisons were made with existing correlations developed with similar storage media. The maximum temperature for the bed was about 1000°C (1830°F) with flue gas as the operating fluid in the storage mode and atmospheric air in the recovery mode. Because most related previous studies were not necessarily focused on high-temperature applications, the published gas-particle heat transfer correlations were obtained at relatively low temperature ranges, generally at room temperature or at temperatures slightly above room temperature. Moreover, only a few of the previously reported correlations associated the results with the corresponding uncertainty margins. The results from this study give a convective gas-particle heat transfer correlation for high-temperature thermal energy storage applications. Also, due to substantial uncertainties normally associated with the measurements of this heat transfer coefficient, it is significant to note that no firm conclusions can be reached on the validity or non-validity of previously reported related correlations for which the uncertainty margins were not reported.

Keywords: Heat transfer coefficient; High temperature; Uncertainty analysis; Packed bed; Thermal energy storage; Heat transfer correlation

1. Introduction

Considerable research has been done on heat transfer in packed beds for thermal energy storage, with interests ranging from theoretical to experimental investigations. Previous related studies by the authors (Adebiyi et al. [1,2]) were mainly on computer simulations involving modeling of a packed bed for thermal energy storage that led to the development of a comprehensive computer model for the sensible heat storage media and parametric studies using the model. During these studies, it was observed that reliable heat transfer correlations for the high-temperature packed bed were hard to come by in the literature. Most of the developed correlations were obtained using spherical particles. The present study is on experimental measurements of the convective gas-pellet heat transfer coefficient in the packed bed, high-temperature, thermal energy storage system utilizing cylindrical pellets.

Relevant previous studies include that of Colburn [3] whose work involved the determination of the coefficients of heat transfer to air flowing through a tube filled with granular materials. The particles were maintained at constant temperature for the duration of the experiments. Lof and Hawley [4] reported the results of an experiment to investigate the unsteady heat transfer between air and loose solids, and presented design data in the form of unsteady-state heat transfer coefficients from air to a 254 mm (10 in.) by 279 mm (11 in.) bed of

* Corresponding author. Tel.: +1-618-453-7021; fax: +1-618-453-7658.
E-mail address: nsofor@engr.siu.edu (E.C. Nsofor).

0894-1777/01/$ - see front matter
PII: S0894-1777(00)00047-9

Nomenclature

A	area (m^2)
A_p	surface area of pellet or particle (m^2)
B	bias uncertainty (dimensionless)
c	specific heat (J/kg K)
D	diameter (m)
G	superficial mass velocity (kg/m^2 s)
h	convective gas-pellet heat transfer coefficient (W/m^2 K)
k	thermal conductivity (W/m K)
L	bed length (m)
l	pellet length (m)
M	total mass of pellets in the bed (kg)
m	mass of pellet (kg)
$\dot{m}$	fluid mass flow rate (kg/s)
N	number (dimensionless)
n	integer used for discretization (dimensionless)
$Nu_{D_p}[= hD_p/k_f]$	the Nusselt number for gas-particle heat transfer (dimensionless)
P	precision uncertainty (dimensionless)
$Pr_f[= \mu_f(c_p)_f/k_f]$	Prandtl number (dimensionless)
T	temperature (°C)
t	time (s)
U	uncertainty (dimensionless)
V	volume of metal pellet (m^3)
W	velocity (m/s)
X	characteristic length (m)

Greeks

Δ	refers to change (dimensionless)
ε	porosity or void fraction (dimensionless)
μ	dynamic viscosity coefficient (kg/m s)
ρ	density (kg/m^3)

Subscripts

1	refers to initial or first
2	refers to final or second
B	refers to bed
e	equivalent
f	fluid or gas
i	initial or first
p	refers to particle
s	refers to solid or metal pellet
t	refers to total number of pellets

granitic gravel. The size of gravel used in the bed of rectangular cross-section ranged from 8 (0.315 in.) to 33.3 mm (1.31 in.), with temperatures ranging from 38°C (100°F) to 121°C (250°F). Bird et al. [5] gave a set of heat transfer correlations for the packed bed which are applicable to the case when the particles are cylindrical.

An attempt at investigations at relatively high temperatures was made by Chen and Churchill [6] in a bid to compare the contribution of radiation and conduction to heat transfer in a packed bed without fluid flow using variables such as shape and size of packing, packing material, porosity, and temperature. Spherical particles of glass, alumina, steel, lead and silicon carbide whose diameters ranged from 1.8 (0.07 in.) to 6.6 mm (0.26 in.) were used in the investigation, with temperatures ranging from 427°C (800°F) to 1093°C (2000°F). Yagi et al. [7] carried out heat transfer measurements employing three sizes of glass spheres and one size of steel balls in packed beds through which water was flowing. The diameter of these spheres and balls ranged from 2.25 (0.09 in.) to 6.38 mm (1/4 in.).

A method of measuring the convective heat transfer coefficient in a packed bed for various packings based on the iterative solution of a mathematical model describing unsteady state heat transfer in fixed beds was presented by Handley and Heggs [8]. The temperatures for the experiments were approximately ambient, and the maximum cylinder size for which a correlation was given was 6.35 mm (1/4 in.) diameter by 12.7 mm (1/2 in.). Littman et al. [9] reported on experiments performed in order to obtain data for the gas-particle heat transfer coefficient in packed beds at low Reynolds numbers using small size spherical particles of copper, lead and glass ranging from 0.5 (0.02 in.) to 2 mm (0.08 in.) diameter.

Bradshaw et al. [10] studied the heat transfer between air and nitrogen in packed beds that led to the presentation of overall heat transfer correlations in terms of the Chilton–Colburn j-factor for packed beds of solids. Alumina, steel and hematite spherical pellets were used in the experiments, and Reynolds number ranged from 150 to 600 with a maximum temperature of 800°C. Wakao et al. [11] proposed heat transfer correlations for both spherical and cylindrical particles based on published heat transfer data obtained from measurements with corrections for the axial fluid thermal dispersion coefficient values.

Jingzhu et al. [12] measured particle-to-gas heat transfer coefficients from one-shot thermal responses in packed beds using spherical glass beads, with air as the operating fluid. The Reynolds number range was 5–229 and temperatures were below 100°C (212°F). Galloway and Sage [13] using spherical pellets based on steady-state conditions developed a correlation for the gas-particle heat transfer coefficient, and later, the constants were modified by Beasely and Clark [14] from measured data. The experimental measurements were for a bed of spherical pellets of soda lime glass 12.6 mm (0.495 in.) in diameter with air as the working fluid. Operating temperatures for the bed was relatively low (less than 100°C (212°F)), and the experimental results presented for heat recovery from the bed were only for the counter-flow process.

Nasr et al. [15] reported the results of experimental study of forced convection heat transfer from a cylinder in a packed bed of spherical particles. Packing materials of aluminum, alumina, glass and nylon were employed

with air as the working fluid. The temperature in the bed was low (about 10°C above inlet ambient air). Uncertainty analysis results presented showed that the uncertainty in the reported Nusselt numbers was ±20.5%.

Previous studies on the gas-particle heat transfer in packed beds have varying differences from this study. These include operations using gases at constant temperature, use of relatively small sizes of spherical pellets and beds and low media temperature conditions. Because most of the studies were not necessarily focused on high-temperature applications, effects such as fluid and solid property variations with temperature appear not to be reflected. Uncertainty analysis which is an important aspect of experimentation was not shown in many of the reports. Only a few associated the results with the corresponding uncertainty margins. This study is on experimental measurements of the convective gas-particle heat transfer coefficient in a packed bed, high-temperature energy storage system utilizing cylindrical pellets of zirconium oxide (ZrO_2) as the sensible heat storage media in the bed. Special attention was paid to uncertainty analysis because the possible experimental methods examined for the determination of the heat transfer coefficient indicated that there would be very high uncertainty margins in the results if proper precautions are not taken in the experimental procedure. The experimental data reduction program written and used in this study incorporated the uncertainty analysis and expressly allowed for media property variations with temperature. The operating fluids in this study were flue gas for the storage of heat and ambient air for the recovery. This brings it closer to applications that can exploit industrial waste flue gas thermal energy. A large percentage of related previous reports employed air as the operating fluid for both heat storage and recovery.

2. Experimental facility and procedure

2.1. Experimental facility

The major components of the experimental facility were the burner, the test section, the cooling station, the main intake/exhaust fan, the combustion air fan, the blower fan, and instrumentation and control devices. Figs. 1 and 2 show the facility in a schematic form. The system can be operated in three modes – storage, counter-current (counterflow) recovery and co-current recovery. These were effected by the opening or closing of appropriate shut-off valves. Details of the test section are shown in Fig. 3. During heat storage, flue gas generated from the gas-fired 350 kW (1.2 MMBtu/h) burner flowed through the test section where heat energy was stored and then to the cooling station, after which it was exhausted by means of the main intake/exhaust fan. Heat recovery was achieved either in co-current recovery or in counter-current recovery depending on whether the direction of flow was the same or opposite to that during storage. In the co-current heat recovery, the burner was shut off while ambient air was made to flow through the

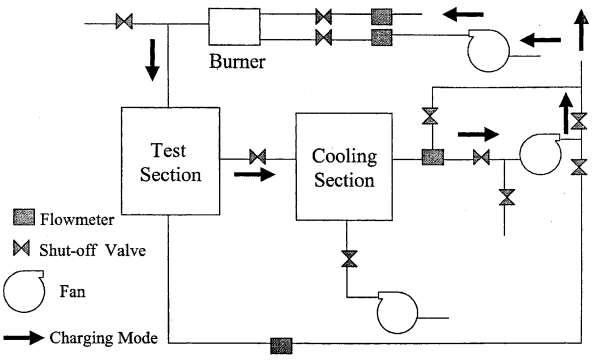

Fig. 1. Schematic of the test facility (charging mode).

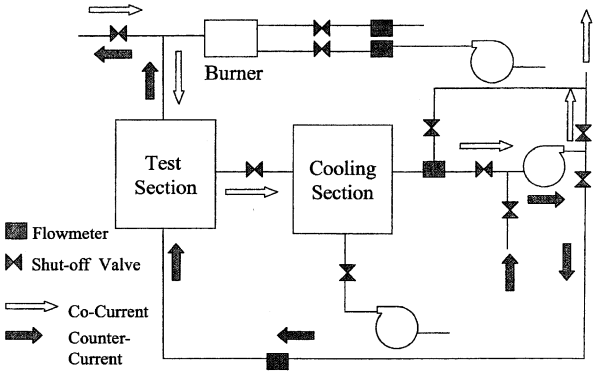

Fig. 2. Heat recovery (co-current and counter-current).

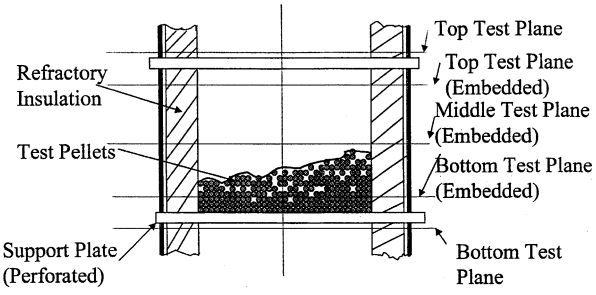

Fig. 3. Details of the test section.

test section from the air intake upstream, thus transferring thermal energy from the bed to the air. In the counter-current heat recovery, the main intake/exhaust fan was used to induce air flow from a secondary supply through the test section in a counterflow mode.

The test section (Fig. 3) which contained the pellets, was an insulated cylindrical vessel with ports at the wall for the insertion of probes for measurements at five test levels along its length. The pellets were actually very short cylinders with slight hemispherical end caps for which an equivalent diameter was determined. The pellets in the bed rested on a perforated inconel plate which was supported by a stack of fire-bricks and a stainless steel stand that rested on the bottom of the

containment cylinder. The ceramic wall was 152-mm (6-in.) thick and made of a castable high alumina refractory-Ladle line. The cooling station contained brick scraps which provided a thermal mass that extracted heat energy from the gas prior to the main intake/exhaust fan. The blower fan cooled the bricks in the cooling station through a secondary loop.

2.2. Experimental procedure

Data acquisition was achieved by means of a personal computer based on a 16-channel A/D interface signal conditioning board. Input signals to the board were either from pressure transducers or thermocouples. Time measurements were obtained from the internal clock in the computer. Thermocouples used were suitable for the range of temperatures encountered in the experiments. Although the thermocouples were precalibrated by the manufacturer, calibration and qualification tests were performed using the Techne calibrator [16]. Pressure measurements were carried out by means of electronic pressure transducers. Flow rates were measured with orifice plates and annubar flowmeters.

The control devices in the experimental facility utilized appropriate sensors to monitor critical physical variables. The speed of the main intake/exhaust fan was controlled by means of a variable frequency drive. This to a large extent controlled the flow rate through the test bed. The system contained a number of shut-off valves designed to effect the mode of operation, i.e., storage, co-current recovery, and counter-current recovery. The main intake/exhaust valve was controlled by means of a motorized actuator. Other controlled devices included the burner and the motorized valves. There were suitable burner safety controls designed to shut off the natural gas supply and activate audible and visual alarms in case of anomalies in the system operation. Nsofor [17] has a more detailed description of the major aspects of the experimental planning, facility and procedure.

For each set of experiments, the test section was filled with the pellets of zirconium oxide poured randomly up to a height of 610 mm (2 ft) above the perforated support plate. The inside diameter of the bed was about 610 mm (2 ft). The choice of this diameter was made in order to have a bed diameter to pellet diameter ratio sufficient to ensure minimal effect of the wall. We estimated the porosity in the bed using Eq. (15) to be about 0.32. Because randomly packed beds show higher values of porosity near the wall due to wall effects, we used a liner on the inside wall to reduce this effect. Handley and Heggs [8] used a similar method to minimize the excess void fraction near the wall. The liner material (12.7 mm (0.5 in.) thick) that we used was fiberfrax durablanket which has a maximum service temperature limit of 1780°C (3236°F). This material is flexible enough to allow the pellets to be slightly embedded, thereby reducing the excess porosity or void fraction. It is a thermal ceramic fiber insulating material that combines the advantages of low heat storage and resistance to thermal shock. The use of this liner helped to bring the test bed much closer to the case of radial uniform porosity. Fig. 3 shows the details of the test section and the test levels.

A very high thermal conductivity metal (copper) pellet of the same shape and approximate size as those in the test bed was instrumented to include a thermocouple to measure its temperature in the bed. Another thermocouple located beside the pellet measured the gas temperature. Time varying inlet temperature gas from the burner was fed at the top of the bed, and temperature measurements were recorded at chosen time intervals as the gas flowed through the bed. Several experimental runs were carried out such that a thermal cycle was completed in each run. A thermal cycle involved heat storage in the bed for a given storage time followed by the removal of heat from the bed in a given recovery time. At the end of storage, the gas inlet temperature to the bed typically reached a peak of about 1000°C (1832°F) while the exit temperature typically reached a peak of about 760°C (1400°F). Thermocouple data were collected via the data acquisition system.

Thermocouple data were reduced by means of the data reduction computer program. The experimental equations developed and uncertainty analysis were incorporated in the computer program and allowance was made for media property variations with temperature. Table 1 presents a summary of the physical and operating parameters with the estimated uncertainties.

Table 1
Summary of parameters with their uncertainties

Parameter	Symbol	Nominal value	Uncertainty
Bed length	L	0.61 m (24 in.)	0.025 m (1.0 in.)
Bed inside diameter	D	0.61 m (24 in.)	0.013 m (0.5 in.)
Void fraction	ε	0.32 m	13.6%
Pellet diameter	D_p	18.3 mm (0.72 in.)	0.38 mm (0.015 in.)
Pellet length	l	18.3 mm (0.72 in.)	0.38 mm (0.015 in.)
Total mass of pellets	M	650.3 kg (1433.7 lbm)	2.3 kg (5 lbm)
Mass flow rate	$\dot{m}$	100–610 kg/h (250–1350 lbm/h)	14 kg/h (30 lbm/h)
Metal pellet density	ϱ_s	8933 kg/m^3 (557.7 lbm/ft^3)	1%
Metal pellet thermal conductivity	k_s	399 W/m K (231 Btu/hr ft R)	1%
Metal pellet specific heat	c_s	402 J/kg K (0.096 Btu/lbm R)	1%
Fluid viscosity	μ_f	3.62×10^{-5} kg/m s (0.243×10^{-4} lbm/ft s)	1%

3. Governing equations and uncertainty analysis

The basis for the instrumented copper pellet used for the measurement of the gas-pellet heat transfer coefficient in the bed is the lumped capacitance heat transfer assumption. This assumption implies that temperature gradients within the metal pellet are negligible at any instant during the transient process. We computed the Biot number for the metal pellet and found this to be very low (about 0.004) for the anticipated scope of the experiments. The value of the thermal conductivity of the metal and dimensions of the cylindrical pellet (of aspect ratio = 1) are shown in Table 1.

The transient response for the metal pellet is determined from the following equation:

$$\varrho_s c_s V \frac{dT_s}{dt} = hA_s(T_f - T_s) \tag{1}$$

from which the expression for h was obtained as

$$h = \left(\frac{\varrho_s c_s V}{A_s}\right)\left(\frac{[T_s(t_2) - T_s(t_1)]}{\int_{t_1}^{t_2}(T_f - T_s)\,dt}\right). \tag{2}$$

It is to be noted that since the aspect ratio (l/D_p) of the cylindrical pellet is 1, then

$$\frac{V}{A_s} = \frac{D_e}{6}.$$

Substituting into Eq. (2) gives

$$h = \left(\frac{\varrho_s c_s D_e}{6}\right)\left(\frac{[T_s(t_2) - T_s(t_1)]}{\int_{t_1}^{t_2}(T_f - T_s)\,dt}\right). \tag{3}$$

If n is an integer used for discretization in time, $t = \Delta n t$, and so,

$$h = \left(\frac{(1.5)^{\frac{1}{3}} D_p \varrho_s c_s}{6}\right)\left(\frac{T_s^n - T_s^1}{\sum_1^n (T_f - T_s)\Delta t}\right). \tag{4}$$

This is the data reduction equation for the gas-particle heat transfer coefficient.

Uncertainty analysis was carried out based on the methods described in [18]. The general uncertainty analysis expression is

$$\left(\frac{U_h}{h}\right)^2 = \left(\frac{U_{\varrho_s}}{h}\frac{\partial h}{\partial \varrho_s}\right)^2 + \left(\frac{U_{c_s}}{h}\frac{\partial h}{\partial c_s}\right)^2 + \left(\frac{U_{D_p}}{h}\frac{\partial h}{\partial D_p}\right)^2 + \left(\frac{U_{T_s^n}}{h}\frac{\partial h}{\partial T_s^n}\right)^2 + \left(\frac{U_{T_s^1}}{h}\frac{\partial h}{\partial T_s^1}\right)^2 + \left(\frac{U_{T_f}}{h}\frac{\partial h}{\partial T_f}\right)^2 + \left(\frac{U_{T_s}}{h}\frac{\partial h}{\partial T_s}\right)^2 + \left(\frac{U_{\Delta T}}{h}\frac{\partial h}{\partial \Delta T}\right)^2. \tag{5}$$

The various measurements of T_f and T_s are correlated. Using the expression by Coleman and Steele [18] gives the expression for the bias limit as

$$\left(\frac{B_h}{h}\right)^2 = \left(\frac{B_{\varrho_s}}{h}\frac{\partial h}{\partial \varrho_s}\right)^2 + \left(\frac{B_{c_s}}{h}\frac{\partial h}{\partial c_s}\right)^2 + \left(\frac{B_{D_p}}{h}\frac{\partial h}{\partial D_p}\right)^2 + \left(\frac{B_{T_s^n}}{h}\frac{\partial h}{\partial T_s^n}\right)^2 + \left(\frac{B_{T_s^1}}{h}\frac{\partial h}{\partial T_s^1}\right)^2 + 2\left(\frac{\partial h}{\partial T_s^n}\right)\left(\frac{\partial h}{\partial T_s^1}\right)B_{T_s^n}B_{T_s^1} + \left(\frac{B_{\Delta T}}{h}\frac{\partial h}{\partial \Delta T}\right)^2 + \sum_{i=1}^{n}\left[\left(\frac{B_{T_{f_i}}}{h}\frac{\partial h}{\partial T_{f_i}}\right)^2 + \sum_{k=i}^{j}\left(\frac{\partial h}{\partial T_{f_i}}\right)\left(\frac{\partial h}{\partial T_{f_k}}\right)B_{T_{f_i}}B_{T_{f_k}}(1-\delta_{ik})\right] + \sum_{i=1}^{n}\left[\left(\frac{B_{T_{s_i}}}{h}\frac{\partial h}{\partial T_{s_i}}\right)^2 + \sum_{k=i}^{j}\left(\frac{\partial h}{\partial T_{s_i}}\right)\left(\frac{\partial h}{\partial T_{s_k}}\right)B_{T_{s_i}}B_{T_{s_k}}(1-\delta_{ik})\right], \tag{6}$$

where Kronecker delta $\delta_{ik} = 1$ for $i = k$ and $\delta_{ik} = 0$ for $i \neq k$

$B_{T_{f_i}} = B_{T_{f_k}} = B_{T_{s_i}} = B_{T_{s_k}} =$ Bias of the thermocouples.

For the precision limit the resulting equation is

$$\left(\frac{P_h}{h}\right)^2 = \left(\frac{P_{\varrho_s}}{h}\frac{\partial h}{\partial \varrho_s}\right)^2 + \left(\frac{P_{c_s}}{h}\frac{\partial h}{\partial c_s}\right)^2 + \left(\frac{P_{D_p}}{h}\frac{\partial h}{\partial D_p}\right)^2 + \left(\frac{P_{T_s^n}}{h}\frac{\partial h}{\partial T_s^n}\right)^2 + \left(\frac{P_{T_s^1}}{h}\frac{\partial h}{\partial T_s^1}\right)^2 + \left(\frac{P_{T_f}}{h}\frac{\partial h}{\partial T_f}\right)^2 + \left(\frac{P_{T_s}}{h}\frac{\partial h}{\partial T_s}\right)^2 + \left(\frac{P_{\Delta T}}{h}\frac{\partial h}{\partial \Delta T}\right)^2 \tag{7}$$

The uncertainty in the gas-pellet heat transfer coefficient was obtained by combining the bias and precision limits using the root-sum-square (RSS) model

$$\frac{U_h}{h} = \left[\left(\frac{B_h}{h}\right)^2 + \left(\frac{P_h}{h}\right)^2\right]^{1/2}. \tag{8}$$

3.1. Reynolds number for flow in the bed

Reynolds number for flow through the packed bed can be defined as

$$Re = \frac{\varrho_f W X}{\mu_f}.$$

If there are N particles and A is the cross-sectional area of the cylindrical bed, then

$$X = \frac{\text{volume of bed}}{\text{total particle surface area}} = \frac{LA}{NA_p}.$$

Also, $NV = (1-\varepsilon)LA$ or $NV = (1-\varepsilon)XNA_p$. This implies that

$$X = \frac{V}{A_p(1-\varepsilon)}.$$

For cylindrical storage particles having an aspect ratio of 1, equivalent spherical particles of diameter D_e may be assumed such that the volumes are the same (Solomon [19]). Equating the volumes of the cylindrical particle and the equivalent spherical particle [1] gives

$$D_e = (1.5)^{1/3} D_p.$$

For this pellet,

$$\frac{V}{A_p} = \frac{\frac{4}{3}\pi\left(\frac{D_e}{2}\right)^3}{4\pi\left(\frac{D_e}{2}\right)^2} = \frac{D_e}{6}.$$

Therefore,

$$X = \frac{D_e}{6(1-\varepsilon)}.$$

We also note that the superficial mass velocity is $G = \rho W$. Therefore, for the packed bed, Reynolds number is given by

$$Re_{D_e} = \frac{GD_e}{6(1-\varepsilon)\mu_f}, \tag{9}$$

where G is obtained from the relationship

$$G = \frac{\text{fluid mass flow rate through the bed}}{\text{frontal area of the bed}},$$

$$G = \frac{\dot{m}}{\frac{\pi D^2}{4}} = \frac{4\dot{m}}{\pi D^2}.$$

When we substitute the values of G and D_e into Eq. (9), the data reduction equation for Reynolds number is

$$Re_{D_e} = \frac{2(1.5)^{1/3} D_p \dot{m}}{3\pi D^2 (1-\varepsilon)\mu_f}. \tag{10}$$

The general uncertainty analysis expression is

$$\left(\frac{U_{Re_{D_e}}}{Re_{D_e}}\right)^2 = \left(\frac{U_{D_p}}{D_p}\right)^2 + 4\left(\frac{U_D}{D}\right)^2 + \left(\frac{U_\varepsilon}{1-\varepsilon}\right)^2 + \left(\frac{U_{\mu_f}}{\mu_f}\right)^2 + \left(\frac{U_{\dot{m}}}{\dot{m}}\right)^2. \tag{11}$$

For the bias limit, the equation for the uncertainty expression is

$$\left(\frac{B_{Re_{D_e}}}{Re_{D_e}}\right)^2 = \left(\frac{B_{D_p}}{D_p}\right)^2 + 4\left(\frac{B_D}{D}\right)^2 + \left(\frac{B_\varepsilon}{1-\varepsilon}\right)^2 + \left(\frac{B_{\mu_f}}{\mu_f}\right)^2 + \left(\frac{B_{\dot{m}}}{\dot{m}}\right)^2. \tag{12}$$

Similarly, for the precision limit, the resulting uncertainty expression is

$$\left(\frac{P_{Re_{D_e}}}{Re_{D_e}}\right)^2 = \left(\frac{P_{D_p}}{D_p}\right)^2 + 4\left(\frac{P_D}{D}\right)^2 + \left(\frac{P_\varepsilon}{1-\varepsilon}\right)^2 + \left(\frac{P_{\mu_f}}{\mu_f}\right)^2 + \left(\frac{P_{\dot{m}}}{\dot{m}}\right)^2. \tag{13}$$

The RSS model for Reynolds number is

$$\frac{U_{Re_{D_e}}}{Re_{D_e}} = \left[\left(\frac{B_{Re_{D_e}}}{Re_{D_e}}\right)^2 + \left(\frac{P_{Re_{D_e}}}{Re_{D_e}}\right)^2\right]^{1/2}. \tag{14}$$

3.2. Porosity

This is determined from the relationship

$$\varepsilon = \frac{\text{fluid volume}}{\text{bed volume}} = \frac{\text{bed volume} - \text{volume occupied by pellets}}{\text{bed volume}}. \tag{15}$$

The volume occupied by the pellets was determined from the relationship

$$V_t = \frac{M}{\varrho_t}.$$

3.3. Uncertainty in the Nusselt number

The data reduction equation for the gas-pellet heat transfer Nusselt number is

$$Nu_{D_e} = \frac{hD_e}{k_f} = \frac{(1.5)^{1/3} h D_p}{k_f}. \tag{16}$$

For the bias limit, the resulting equation is

$$\left(\frac{B_{Nu_{D_e}}}{Nu_{D_e}}\right)^2 = \left(\frac{B_h}{h}\right)^2 + \left(\frac{B_{D_p}}{D_p}\right)^2 + \left(\frac{B_{k_f}}{k_f}\right)^2. \tag{17}$$

For the precision limit, the resulting expression is

$$\left(\frac{P_{Nu_{De}}}{Nu_{De}}\right)^2 = \left(\frac{P_h}{h}\right)^2 + \left(\frac{P_{D_p}}{D_p}\right)^2 + \left(\frac{P_{k_f}}{k_f}\right)^2, \tag{18}$$

and the RSS model in this case is

$$\left(\frac{U_{Nu_{D_e}}}{Nu_{D_e}}\right)^2 = \left(\frac{B_{Nu_{D_e}}}{Nu_{D_e}}\right)^2 + \left(\frac{P_{Nu_{D_e}}}{Nu_{D_e}}\right)^2. \tag{19}$$

These equations for Nusselt number and gas-particle heat transfer coefficient (h) along with related parameters were used in data reduction for experimental planning and procedure. The uncertainties in the experimental data were estimated at 95% confidence level. Table 1 gives a summary of the physical and operating parameters with the estimated uncertainties.

4. Results and discussion

In the development of the gas-pellet heat transfer Nusselt number correlation, it was noted that all the related existing correlations are functions of Reynolds number and Prandtl number. Some of these existing correlations involving cylindrical particles are examined in the following.

(a) Wakao et al. [11]

$$Nu_{D_p} = 2.0 + 1.1[6(1-\varepsilon)]^{0.6} Re_{D_p}^{0.6} Pr_f^{1/3}. \tag{20}$$

This correlation was obtained based on published empirical data for spherical and cylindrical particles for Reynolds number (Re_{D_p}) range 4–2100.

(b) Incropera and DeWitt [20]

$$Nu_{D_p} = \frac{0.79}{\varepsilon}[6(1-\varepsilon)]^{0.425} Re_{D_p}^{0.425} Pr_f^{1/3}. \quad (21)$$

This is for a bed of cylindrical particles. The range of Reynolds number (Re_{D_p}) for this is 20–1000.

(c) Bird et al. [5]

$$Nu_{D_p} = 0.789[6(1-\varepsilon)] Re_{D_p}^{0.49} Pr_f^{1/3} \quad (22)$$

for Reynolds number less than 45, and

$$Nu_{D_p} = 0.534[6(1-\varepsilon)] Re_{D_p}^{0.59} Pr_f^{1/3} \quad (23)$$

for Reynolds number greater than 45.

These correlations are for packed beds utilizing cylindrical particles. Also, the operations fall within the same Reynolds number range as those covered in this study.

As suggested by the existing correlations above, the decision was taken in this study to correlate the Nusselt number as a function of Reynolds number and Prandtl number in the form

$$Nu_{D_p} = b + a_1[6(1-\varepsilon)]^{a_2} Re_{D_p}^{a_2} Pr_f^{1/3}, \quad (24)$$

where a_1, a_2, and b are empirical constants determined from fitting of the experimental data. Eq. (24) was chosen after considering different types of relations that fitted the experimental data best.

The non-linear regression Curve Fit Function in the SigmaPlot software package (SigmaPlot Scientific Graph System) was used for the curve-fitting. This function fits equations to data which are non-linear functions of their parameters and determines the best parameters to fit a curve to the data. The algorithm involved determines the parameters that minimize the sum of the squares of differences between the dependent variables in the equation and the observation.

The result obtained for the gas-pellet heat transfer was

$$Nu_{D_p} = 8.74 + 9.34[6(1-\varepsilon)]^{0.2} Re_{D_p}^{0.2} Pr_f^{1/3}. \quad (25)$$

Fig. 4 shows the plot of Nusselt number versus Reynolds number for a typical experimental run compared with data generated using the new correlation for the same experimental conditions. The limits of the experimental uncertainties are also shown. The figure shows that the correlation generally fits the experimental values, especially as Reynolds number increases. Eq. (25) was the single best equation that represents data from the experiments. The multiple correlation coefficient squared was 0.957. Fig. 5 is the plot of Nusselt number versus Reynolds number for the correlation developed in this study compared with some of the published correlations for cylindrical pellets for a typical set of experimental data. The experimental data ranged from values for relatively low temperatures (less than 200°C) to high temperatures (400–1000°C). The figure shows that at low temperatures, there is reasonable agreement between the developed correlation and Wakao et al. [11]. A likely explanation for the difference seen between them at high temperatures is the fact that the present study includes high-temperature operations and incorporates media property variations with temperature. This comparison was made because the results from Wakao et al. [11] were obtained from a much wider study than the others, as several published empirical data were used to develop the correlation.

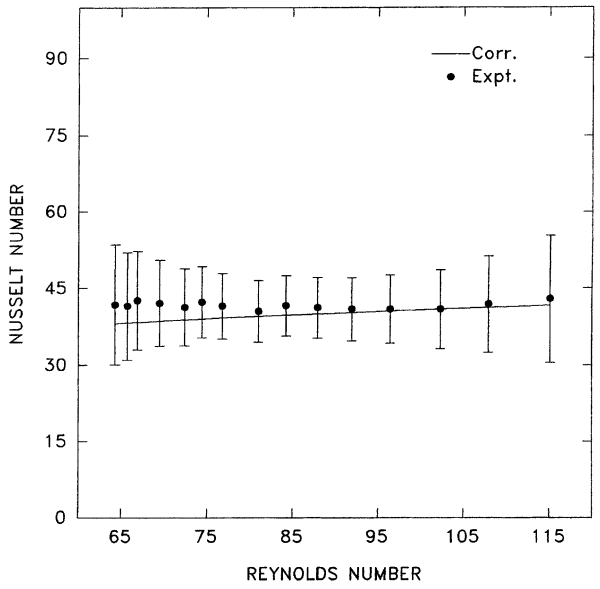

Fig. 4. Nusselt number versus Reynolds number (experiment data compared with new correlation for the same experimental conditions).

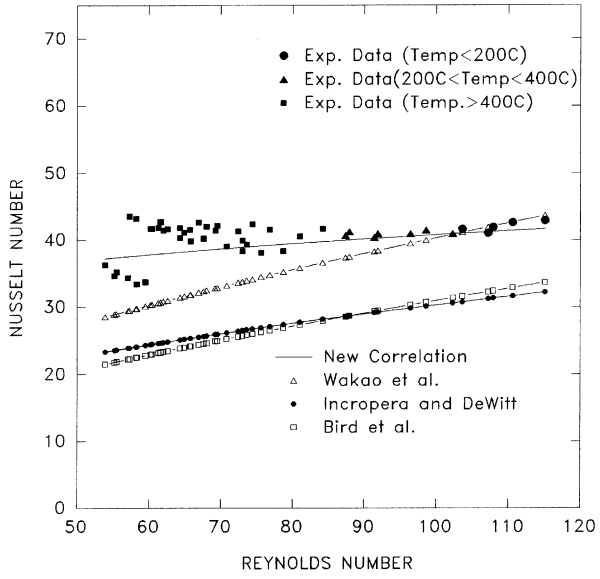

Fig. 5. Existing gas-pellet heat transfer correlations compared with the resulting correlation from this study.

5. Practical significance/usefulness

The operation of the packed bed for energy storage depends upon efficient heat transfer between the fluid stream and the solid particles in the bed. Heat transfer characteristics for packed beds operating at high temperatures are important for the design of waste heat recovery systems, fuel beds, heat regenerators, solar thermal energy utilization, fluidized bed combustion, and similar applications. The industrial countries of the world are today more conscious of their energy requirements and consumption than ever before and to meet the energy challenges, there is a need to explore ways to efficiently utilize available energy. Thermal energy storage devices contribute tremendously to improving the overall efficiency of energy consuming units.

This study has an impact on efficient heat transfer in thermal energy storage devices as it contributes to understanding and quantifying the heat transfer in the packed bed for high-temperature thermal energy storage. The results are useful to the industry engaged in the development of thermal energy storage devices especially those involved in waste heat recovery and solar thermal energy exploitation especially for cases of temperatures in the range of 500–1000°C. There are also potential space applications. Any useful information concerning the laws of heat transfer between a fluid stream and a packed bed is of interest to brick, ceramic, and similar industries.

6. Conclusions

An experimental determination of the forced convection gas-particle heat transfer coefficient in a packed bed for high-temperature thermal energy storage utilizing cylindrical particles is presented. It is noted that existing heat transfer correlations for the packed bed thermal energy storage are limited to relatively low temperature ranges, with the majority obtained near room temperature and with spherical particles. Moreover, the fluid temperatures at the entry to the bed have been reported to be constant in many cases. In this study, the gas-pellet heat transfer correlation for the packed bed thermal energy storage for high temperatures was developed. The results obtained are for temperatures up to 1000°C (1830°F). For this correlation, the fluid temperatures at the inlet to the bed can vary with time.

The gas-pellet heat transfer correlation developed is given by Eq. (25). The range of Reynolds number as defined in this study (Eq. (10)) is 50–120. It is also noted that the uncertainty margin in the heat transfer correlations is normally large. Many previous reported related investigations did not associate their results with the corresponding uncertainty margins. The few that did, indicated large values (usually not less than ±20%). An example is the report by Nasr et al. [15] on an experimental investigation on forced convection heat transfer from a cylinder embedded in a packed bed. The uncertainties in the Nusselt numbers from that study were reported to be ±20.5%. In this study, conscientious efforts were made to ensure that results obtained have uncertainties that were as low as possible. The uncertainty range in the Nusselt number correlation developed is ±10–30%. This range seems high but was not unexpected. The results from this study indicate that due to the substantial uncertainties associated with the measurements of the gas-particle heat transfer coefficient, no firm conclusions can be reached on the validity or non-validity of previously reported correlations for which uncertainty margins are not reported.

It is recommended that further work be aimed at investigations on: (a) flows outside the range of Reynolds number covered by this study; (b) higher media temperatures (i.e. greater than 1000°C); and (c) experimental methods for obtaining lower uncertainty margins in the Nusselt numbers.

Acknowledgements

This study was funded under a contract by the US Department of Energy through the Oak Ridge National Laboratory. The authors gratefully acknowledge this support.

References

[1] G.A. Adebiyi, B.K. Hodge, W.G. Steele, A. Jalalzadeh, E.C. Nsofor, Computer simulation of a high temperature thermal energy storage system employing multiple families of phase change materials, J. Energy Res. Tech. 118 (2) (1996) 102–111.
[2] G.A. Adebiyi, E.C. Nsofor, W.G. Steele, A. Jalalzadeh, Parametric study on the operating efficiencies of a packed bed for high-temperature sensible heat storage, ASME J. Solar Energy Eng. 120 (1) (1998) 2–13.
[3] A.P. Colburn, Heat transfer in empty, baffled and packed tubes, Ind. Eng. Chem. 23 (1931) 910–913.
[4] G.O.G. Lof, R.W. Hawley, Unsteady-state heat transfer between air and loose solids, Ind. Eng. Chem. 40 (1948) 1061–1069.
[5] R.B. Bird, W.E. Stewart, E.N. Lightfoot, Transport Phenomena, Wiley, New York, 1960.
[6] J.C. Chen, S.W. Churchill, Radiant heat transfer in packed beds, Am. Inst. Chem. Eng. J. 9 (1963) 35–41.
[7] S. Yagi, D. Kunii, K. Endo, Heat transfer in packed beds through which water is flowing, Int. J. Heat Mass Transfer 7 (1964) 333–339.
[8] D. Handley, P.J. Heggs, Momentum and heat transfer mechanism in regular shaped packing, Trans. Inst. Chem. Eng. 46 (9) (1968) 251–264.
[9] H. Littman, R.G. Barile, A.H. Pulsifer, Gas-particle heat transfer coefficients in packed beds at low Reynolds numbers, Ind. Eng. Chem. Fund. 7 (4) (1968) 554–561.
[10] A.V. Bradshaw, A. Johnson, N.H. McLachlan, Y.T. Chiu, Heat transfer between air and nitrogen and packed beds of non-reacting solids, Trans. Inst. Chem. Eng. 48 (1970) 77–84.
[11] N. Wakao, S. Kaguei, T. Funazkri, Effect of fluid dispersion coefficients on particle-to-fluid heat transfer coefficients in packed beds, Chem. Eng. Sci. 34 (1979) 325–336.
[12] S. Jingzhu, S. Kaguei, N. Wakao, Measurements of particle-to-gas heat transfer coefficients from one-shot thermal responses in packed beds, Chem. Eng. Sci. 36 (8) (1981) 1283–1286.

[13] T.R. Galloway, B.H. Sage, A model of mechanism of transport in packed, distended and fluidized beds, Chem. Eng. Sci. 25 (1970) 495–516.
[14] D.E. Beasley, J.A. Clark, Transient response of a packed bed for thermal energy storage, Int. J. Heat Mass Transfer 27 (1984) 1659–1669.
[15] K. Nasr, S. Ramadhyani, R. Viskanta, An experimental investigation on forced convection heat transfer from a cylinder embedded in a packed bed, J. Heat Transfer 116 (1) (1994) 73–80.
[16] Dry Block Calibrator System, Davis Instrument Manufacturing Company, Baltimore, MD, 1992.
[17] E.C. Nsofor, Experimental investigations of the convective heat transfer coefficients and computer model calibration involving a high-temperature thermal energy storage system, Ph.D. Dissertation, Mech. Eng. Dept., Miss. State Univ., Mississippi State, MS, 1993.
[18] H.W. Coleman, W.G. Steele Jr., Experimentation and Uncertainty Analysis for Engineers, Wiley, New York, 1989.
[19] A.D. Solomon, Melt time and heat flux for a simple PCM body, Journal of Solar Energy 22 (1979) 251–257.
[20] F.P. Incropera, D.P. DeWitt, Introduction to Heat Transfer, second ed., Wiley, New York, 1990.